



Engineering characterization of ReadyToProcess WAVE 25 bioreactor system with 20 L Cellbag culture chamber

Intellectual Property Notice: The Biopharma business of GE Healthcare was acquired by Danaher on 31 March 2020 and now operates under the Cytiva™ brand. Certain collateral materials (such as application notes, scientific posters, and white papers) were created prior to the Danaher acquisition and contain various GE owned trademarks and font designs. In order to maintain the familiarity of those materials for long-serving customers and to preserve the integrity of those scientific documents, those GE owned trademarks and font designs remain in place, it being specifically acknowledged by Danaher and the Cytiva business that GE owns such GE trademarks and font designs.

cytiva.com

GE and the GE Monogram are trademarks of General Electric Company.
Other trademarks listed as being owned by General Electric Company contained in materials that pre-date the Danaher acquisition and relate to products within Cytiva's portfolio are now trademarks of Global Life Sciences Solutions USA LLC or an affiliate doing business as Cytiva.
Cytiva and the Drop logo are trademarks of Global Life Sciences IP Holdco LLC or an affiliate. All other third-party trademarks are the property of their respective owners.
© 2020 Cytiva
All goods and services are sold subject to the terms and conditions of sale of the supplying company operating within the Cytiva business. A copy of those terms and conditions is available on request. Contact your local Cytiva representative for the most current information.
For local office contact information, visit [cytiva.com/contact](https://www.cytiva.com/contact)



Engineering characterization of ReadyToProcess WAVE™ 25 bioreactor system with 20 L Cellbag™ culture chamber

The knowledge of the engineering parameters of a bioreactor is essential to successfully run a biological production process and to transfer the process to different bioreactors and scales. Here, we describe the characterization of the single-use ReadyToProcess WAVE 25 rocking bioreactor system. Classical engineering methods were used to characterize mixing and oxygen transfer. Computational fluid dynamics (CFD) were used to account for the location-dependent fluid flow pattern.

Introduction

The most important parameters used in the past to compare different types of bioreactor systems are the mixing time t_m (accounting for the ability to achieve a homogeneous culture broth), the power input P/V (accounting for the level of energy brought to the system with inference to the average shear stress), and the oxygen mass transfer coefficient $k_L a$ (accounting for the ability to supply oxygen to the system).

With the help of CFD, the location and time dependency of fluid flows can be determined. Thus, process crucial parameters like shear stress and mixing efficiency can be identified. For a CFD simulation, a 3D computer-aided design (CAD) model is necessary. Therefore, a bag replica out of gypsum was made. Thereafter, a laser scanning and reverse-engineering method was applied to create the 3D model. The CAD model can be used to generate a mesh model out of a large number of control volumes at which the partial differential equations will be discretized. The fluid flow pattern of the ReadyToProcess WAVE 25 was simulated using an open-source CFD software suite (OpenFOAM). From the simulation, fluid flow pattern, velocity profiles, distribution of shear and energy dissipation, specific surfaces, turbulence intensity, etc. were determined and the power input was calculated.

Materials and methods

Engineering characterization

Operating parameters

The engineering characterization was performed in a 20 L Cellbag culture chamber. The working volume was set to the minimal (2 L) and maximal (10 L) levels of the culture bag. The variation of the operating parameters included the rocking rate, rocking angle, and acceleration. Investigations were performed at minimal and maximal values given by the system and at intermediate values thought to be suitable for cell cultures. In Table 1, a detailed overview of the investigated parameters is given. For measurement of the $k_L a$ value, a bag with optical sensors for measurement of dissolved oxygen (DO) was used. Mixing time measurements were accomplished with a basic bag. The mixing time t_m and the $k_L a$ value were determined in duplicate.

Table 1. Operating parameters for engineering characterization of the 20 L Cellbag culture chamber with 2 L and 10 L filling volume

Rocking speed (rpm)	Rocking angle (°)	Acceleration (%)
10	6	15
10	6	100
20	6	15
20	6	50
20	6	100
30	8	15
30	8	50
30	8	100
40	12	15
40	12	100

Mixing time

The measurement of the mixing time was accomplished with the de-colorization method (1). To determine the mixing time, a water-starch solution (5 mL/L) was stained by addition of iodide solution (1 mL/L) for a dark blue starch-iodine complex to form. In the presence of sodium thiosulfate, the complex is reduced, resulting in a de-colorization. As 95% homogeneity is assumed to be the maximum achievable mixing quality in mixing processes, the thiosulfate solution was prepared with a 5% higher concentration than required to completely reduce the starch-iodine complex. After adding the sodium thiosulfate solution, the time was measured until complete de-colorization.

Specific oxygen transfer coefficient ($k_L a$)

Oxygen supply in rocking bioreactors is realized by the wave motion and surface aeration. This way, no bubbles are introduced into the system through spargers. In general, aeration efficiency depends mainly on how the air is transferred into the system (bubble aeration, surface aeration, membrane aeration), but also on the culture volume, aeration rate, and fluid flow in the cultivation system. In different studies, oxygen mass transfer rates for rocking bioreactor systems were determined to be in the range of 1 to 15 h⁻¹ (2, 3).

The oxygen mass transfer rate was determined with the gassing out method. An adapted method was performed in accordance with the Gesellschaft für Chemische Technik und Biotechnologie (DECHEMA) instruction. First, a gassing with air for three hours was performed to equilibrate the DO probe. This allows the fluid to achieve saturation with oxygen, and the calibration at 100% DO can be performed. In the next step, the oxygen is stripped with pure nitrogen. To conduct the $k_L a$ measurement, the rocking of the platform was stopped and the headspace, which was filled with nitrogen, was replaced with air (to set the partial pressure of oxygen in the gaseous phase to the value used within the subsequent $k_L a$ calculation). After five minutes, the rocking was started and the saturation profile was recorded with the UNICORN™ 6.3.2 software. For evaluation of the oxygen mass transfer rate, the transfer equation was linearized. $k_L a$ was calculated where the graph showed linear behavior, typically in the DO range between 20 and 90%.

Computational fluid dynamics

To create a CFD simulation case, the following general procedure is recommended:

- Gather geometry data and generate 3D CAD files
- Generate the mesh
- Run an initial test with most stable parameters for solver and turbulence model

- Adjust to more accurate solver settings and turbulence models
- Run test cases
- Perform qualification of the test cases
- Determine solver setting, turbulence models, and further models
- Establish a convenient and automated work flow for all future simulation cases
- Run parameter study
- Evaluate data

Geometry

Three-dimensional (3D) geometric data were needed for the CFD simulation. To gather geometric data, the 20 L culture bag was filled with body filler (mainly gypsum and methyl cellulose) and dried for two weeks (Fig 1A). The gypsum models were scanned and a 3D CAD model was created by reverse engineering (Fig 1B).

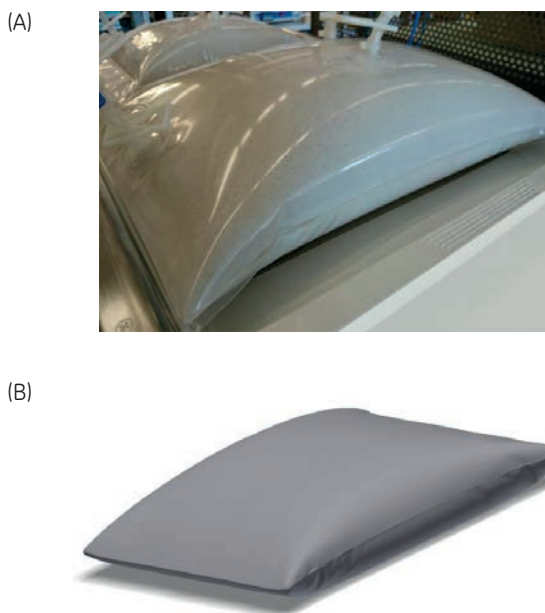


Fig 1. Gathering 3D CAD data for the culture bags: (A) Gypsum model and (B) 3D CAD model.

Meshing

The meshing was accomplished with the command line tool snappyHexMesh included in OpenFOAM 2.3.x. The tool produces high-quality hexagonal mesh elements, which is an important influencing parameter to the accuracy and stability of the numerical solution. First, a blockMesh was created, which completely embeds the geometry from the STL file in all three dimensions. The final mesh size can be either adjusted by the basic blockMesh (which is

recommended especially for complex geometries) or by a refinement of edges (1D), surfaces (2D), and regions (3D) with snappyHexMesh. The patches to define boundary conditions (here: wall) were created by the command line tool autoPatch.

To evaluate the mesh quality, two parameters can be examined: non-orthogonality (angle between the line connecting two cell centers and the normal of their common face) and skewness (distance between the intersection of the line connecting two cell centers with their common face and the center of that face). The main important quality criteria are the non-orthogonality of the mesh cells (below 65°) and the skewness of the mesh cells (below 5). Thus, all following meshes had to fulfill at least these values. A mesh study was accomplished.

Operating parameters

The chosen parameters for the CFD simulations were similar to the parameters of the engineering characterization. A complete overview for all investigated parameters is listed in Table 2.

Table 2. Operating parameters for CFD in the 20 L Cellbag culture chamber with 2 L and 10 L filling volume

Rocking speed (rpm)	Rocking angle (°)	Acceleration (%)
10	6	15
10	6	100
16	6	15
16	6	50
16	6	100
20	6	15
20	6	100
30	8	15
30	8	100
40	12	15
40	12	100

interDyMFoam solver

To simulate the unsteady fluid flow in the moving culture chamber, the interDyMFoam solver from OpenFOAM was used. The interDyMFoam is the solver for two incompressible fluids (air and water) with mesh motion. To solve the Navier-Stokes equations, a two-phase surface compression volume of fluid method (VoF) was used, treating two phases as a single phase with volume fraction ($\alpha \in [0;1]$). The Navier-Stokes equations were solved with those implemented in OpenFOAM time-dependent pressure implicit splitting of operator (PISO) algorithm, where pressure and flux are

assumed using the values from the previous time step. With these values, the velocity can be found from the momentum equation. Afterwards, the pressure equation can be solved and flux corrected to fulfil the continuity.

Rocking motion profile

To simulate movement of fluid, a moving mesh function is needed. The vanilla rotatingMotion function from OpenFOAM was changed in such a way that an oscillatory movement of the fluid volume (culture chamber) is achieved in accordance with the operating parameters of the bioreactor system, defined by the rocking angle, the rocking speed, and the acceleration. To consider the acceleration of the rocking platform, mathematical transformations are required. Rocking angle and rocking rate can be defined as amplitude and frequency of the oscillatory movement. The acceleration can be defined as the smoothing of a triangular oscillatory function. In Figure 2, the smoothing is depicted in blue and the triangular oscillatory function is depicted in red color. The acceleration parameter defines the time of the triangular function, which is smoothed with a cosine function. For example, acceleration of 30% means that 15% of the time the platform is smoothly accelerated, 70% of the time it rotates with constant speed, and the remaining 15% are spent on smooth deceleration.

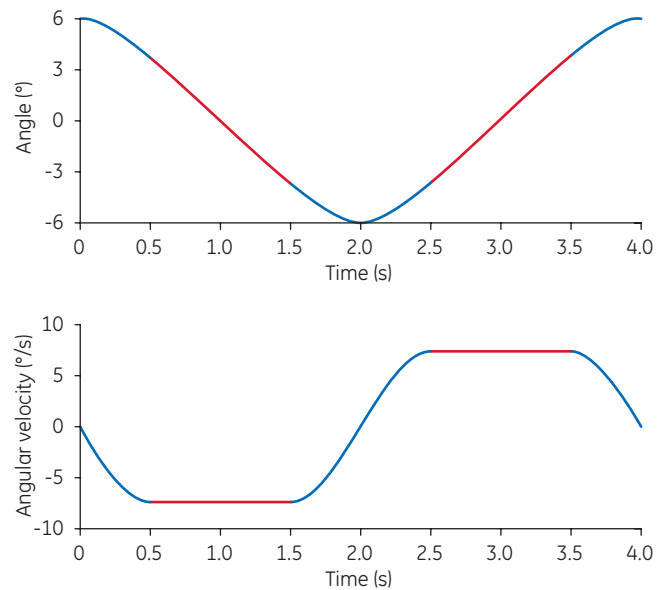


Fig 2. Example of rocking profile 15 rpm, 6° and 50% acceleration. Blue is in ramping up/down (cosine curve) and red is constant speed.

Fluid properties

For the CFD simulations, water and air at 25°C, with a dynamic viscosity μ of 8.84×10^{-4} kg/s/m and 1.86×10^{-5} kg/s/m, respectively, and a kinematic viscosity ν of 8.9×10^{-7} m²/s and 1.55×10^{-5} m²/s, respectively, were used. The density ρ of the fluids were set to 993 kg/m³ and 1.2 kg/m³, respectively.

Calculations for evaluating

A volume average of property Φ in the ReadyToProcess WAVE 25 bioreactor for every time step can be calculated with the following equation:

$$\overline{\Phi}_c = \frac{1}{\sum \alpha_c V_c} \sum \alpha_c V_c \Phi_c$$

where Φ_c is the value of property Φ in cell c ; V_c is the volume of the cell c and α_c is the mass fraction of water in the cell c .

Normal (λ_{nn}) and shear (λ_{nt}) velocity gradients can be calculated using the transformation of the global coordinate system for each cell as described elsewhere (4, 5). Normal and shear components of the hydrodynamic stress can be calculated from normal and shear velocity gradients with the equation:

$$\tau = \mu \gamma$$

The Kolmogorov microscale of turbulence h can be calculated from the turbulent kinetic energy k and the rate of dissipation ω of the turbulent kinetic energy with the following equation:

$$\eta = \left(\frac{\nu^3}{\varepsilon} \right)^{\frac{1}{4}} = \left(\frac{\nu^3}{C_\mu k \omega} \right)^{\frac{1}{4}}$$

with a constant value $C_\mu = 0.09$, which is defined by the turbulence model.

Results

Engineering characterization

The engineering characterization of ReadyToProcess WAVE 25 was performed with water-like fluids at 25°C. The methods to measure the mixing time and oxygen mass transfer coefficient are well defined and verified. The mixing time was determined by the de-colorization method, and the oxygen mass transfer was determined using the dynamic gassing out method for a range of operating parameters.

Determination of mixing time

In this study for the 20 L Cellbag culture chamber with 2 L working volume, the mixing times were in the range of 14 to 104 s (Fig 3). In general, the mixing times decreased with higher rocking rates. At the lowest rocking rate and rocking angle, the mixing was most inefficient with a mixing time of 104 s.

The acceleration showed a slight influence at the lowest rocking rate and rocking angle. However, taking the error bars in consideration, it is shown that the influence can be neglected, in particular with faster rocking speed and larger rocking angle. In the case of the minimal working volume of 2 L, increase in rocking rate was shown to exhibit the largest impact on mixing time.

Similar investigations were conducted with a working volume of 10 L. Again, the increase in rocking rate was shown to impact mixing time most. At this maximal working volume, the mixing time ranged between 7 and 1700 s (Fig 4). At the lowest rocking rate of 10 rpm and 6° angle, the mixing time was reduced from around 1700 s down to 900 s when the acceleration was changed from 100% to 15%. For 20 rpm and 6°, the mixing time at 15% acceleration was 95 s compared with 210 s at 100% acceleration. When the rocking rate was increased from 30 rpm to 40 rpm, a homogeneous condition was achieved within 7 s and 18 s, respectively. This shows that rocking rate and angle influence mixing time most.

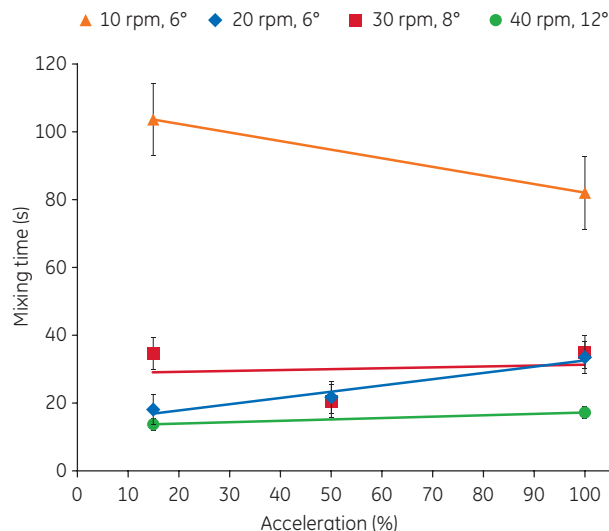


Fig 3. Mixing time with 2 L filling volume.

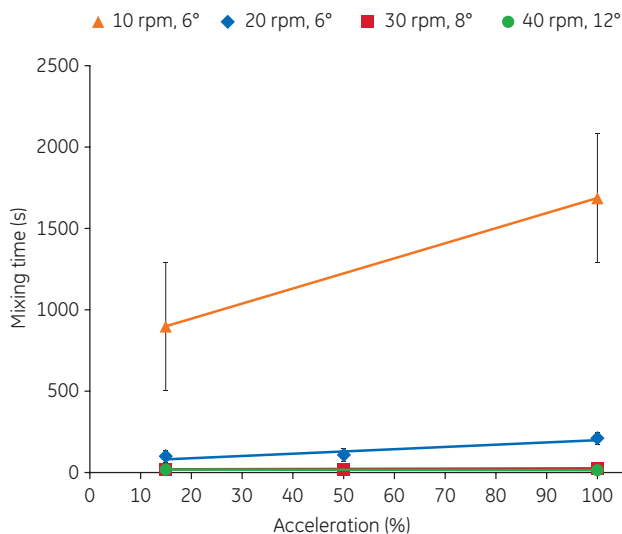


Fig 4. Mixing time with 10 L filling volume.

Typical mixing time for stirred bioreactors is about 20 s (2), whereas for rocking bioreactor systems, the mixing time range is much wider, up to 1400 s (3). It is important to avoid working at very low mixing unless the process requires very gentle mixing, for example, at the very beginning of the cultivation (valid for certain plant and animal cells). In particular at low rocking speed, there is mostly a longitudinal oriented mass transfer and very low meridional mixing occurring.

After adding thiosulfate solution on the left side of the bag, a sharp boundary of blue and colorless fluid could be seen (Fig 5). The meridional de-colorization is mostly driven by diffusion and thus, the mixing time is reduced significantly.



Fig 5. Illustration of the two separate compartments during de-colorization for determination of mixing time in the 20 L Cellbag culture chamber.

When rocking speed was set in the lower range (10 to 20 rpm), the error bars were much wider than at the higher settings (30 and 40 rpm). This can be explained by the unstable fluid flow in the Cellbag culture chamber and the slight variation in thiosulfate addition with respect to timing and wave cycle. These phenomena are well known for a rocking motion (6).

To reduce the mixing time, it is recommended to increase the rocking speed and angle instead of the acceleration in the first place. At a lower rocking speed such as 10 rpm and 20 rpm, changing the acceleration can reduce the mixing time by 50%.

In accordance with the expected correlation of mixing time to specific power input, the mixing time decreased when increasing the power input (Fig 6). When an average power input of 130 W/m³ was reached, the mixing time could not be reduced much further. This was also the case for accelerations of 15% (Fig 6A) and 100% (Fig 6B). The fastest mixing time achievable was around 7 s.

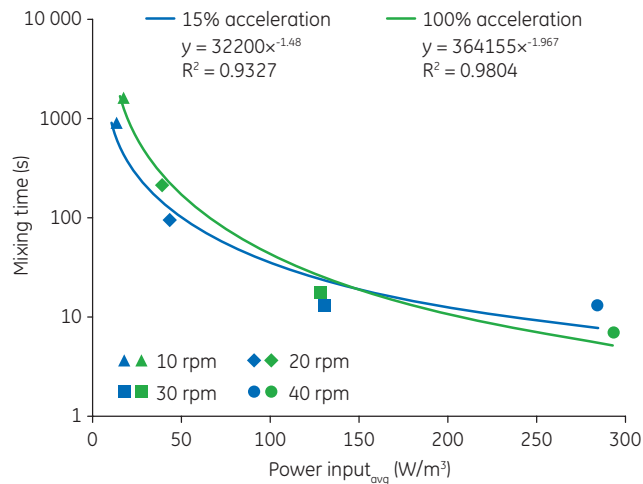


Fig 6. Mixing time compared with the specific power input from the CFD calculations at a working volume of 10 L.

Determination of oxygen mass transfer rate

The oxygen mass transfer rate was determined using identical parameters as for the mixing time investigations. For the lower working volume of 2 L, the measured $k_L a$ values are shown in Figure 7. The oxygen mass transfer rate was determined to be in the range 4.5 to 5.7 h^{-1} . The influence of the acceleration on the oxygen mass transfer rate can be neglected.

In contrast to the mixing time results, the error bars are very narrow. This is mainly due to the fact, that the oxygen is evenly injected; compared with in the mixing time experiments, where the thiosulfate solution needed to be injected to the very exact location on the surface. Furthermore, the measurement of the time was accomplished by computer-based recording of the answer function for the oxygen mass transfer rate determination and measured manually by the operator for the mixing time experiments.

Investigations of the oxygen mass transfer rate for 10 L working volume were performed at the same rocking motion as for 2 L working volume. The results are shown in Figure 8. The range was between 0.5 h^{-1} (at a rocking rate of 10 rpm and a rocking angle of 6°) and 12 h^{-1} (at a rocking rate of 40 rpm and a rocking angle of 12°), which is within the known range for rocking bioreactor systems (3).

Correlating the oxygen mass transfer rate to the specific power input, the oxygen mass transfer rate increases exponentially with increasing specific power input. From 10 to 20 rpm, with doubling of the power input from 20 to 40 W/m^3 , the $k_L a$ value increases six-fold. Increasing the power input further results in a much lower (10 to 12 h^{-1}) increase in oxygen mass transfer rate (Fig 9).

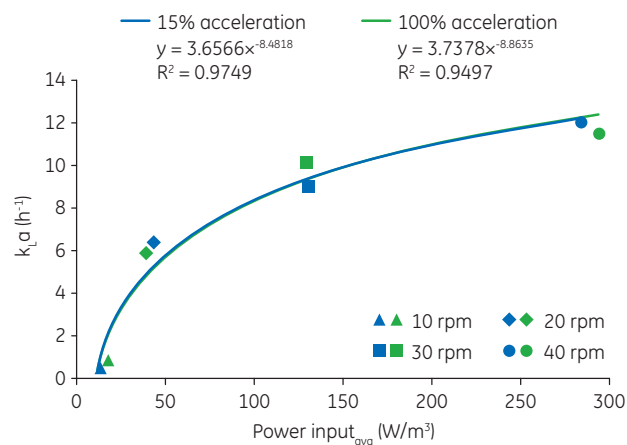


Fig 9. Specific oxygen transfer coefficient compared with the specific power input at 10 L working volume.

Computational fluid dynamics (CFD)

Mesh and solver study

The motion function that was built and added to OpenFOAM to move the culture bag properly, was tested successfully with a basic mesh and was used for all further simulations. To optimize the quality of the results and the calculation time, a mesh size study with cell numbers ranging from 0.1 to 2.5 million cells was accomplished. In Figure 10, it can be seen that the results of the fluid surface distribution for the meshes with less than 1.92 million cells differ significantly from those with 1.92 million and 2.55 million cells. Due to higher calculation costs, the mesh with 1.92 million cells was chosen for all subsequent investigations.

The non-orthogonality and the skewness for the mesh with 1.92 million cells were 60 and 2, respectively, which represents a reasonable quality. Approximately 90% of the cells are hexahedral cells, 6% are polyhedral cells, and 4% are prisms.

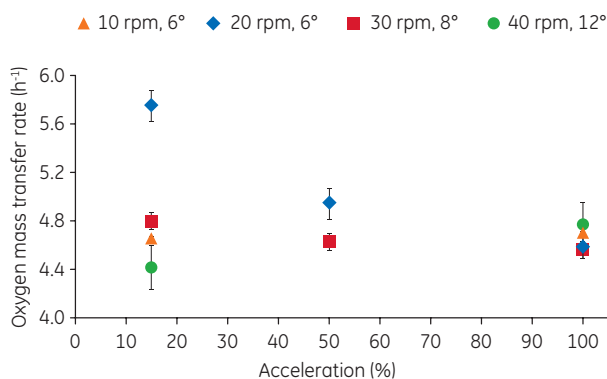


Fig 7. Specific oxygen transfer coefficient with 2 L filling volume.

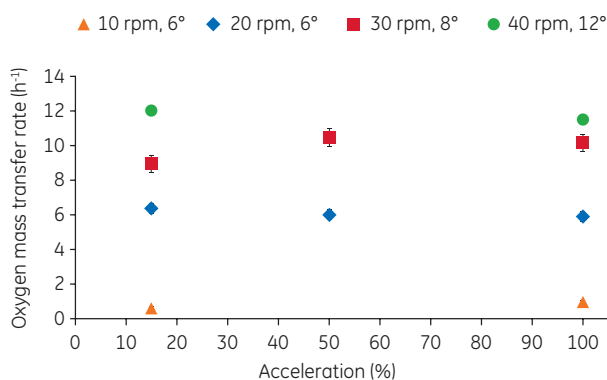


Fig 8. Specific oxygen transfer coefficient with 10 L filling volume.

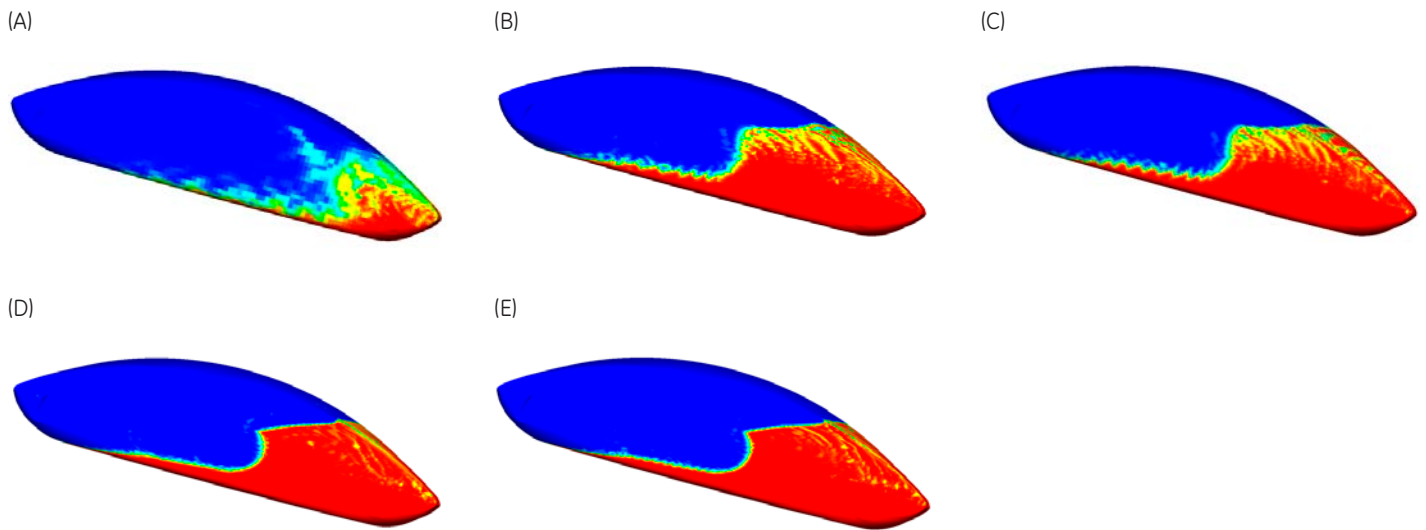


Fig 10. Comparison of CFD-predicted fluid flow pattern in the Cellbag culture chamber with 10 L filling volume for different mesh qualities: (A) 0.11 million cells, (B) 0.67 million cells, (C) 1.06 million cells, (D) 1.92 million cells, and (E) 2.55 million cells.

Selection of thresholds for surface calculation

To calculate the maximum, minimum, and average value of any property Φ in the Cellbag culture chamber, the phase fraction α should be discretized: each cell should be assumed to contain either water or air only. A threshold of 0.5 for α (there is only water in the cell if α is higher than 0.5, otherwise there is only air) provides the best results, in a sense that the total fluid volume in the Cellbag culture chamber is close to constant when computed with the following equation:

$$V_{\text{fluid}} = \sum_c \alpha_c V_c$$

where V_c and α_c are volume of cell c and mass fraction of water in the cell c , respectively. Thus, the threshold to distinguish between water and air within one control volume was set to 0.5 for all subsequent investigations.

Fluid velocity

The CFD-predicted pattern for the magnitude of the fluid velocity in the Cellbag culture chamber at 40 rpm, 12° amplitude, and 100% acceleration with 10 L filling volume are presented in Figure 11 and with 2 L filling volume in Figure 12. The highest velocities were observed at the bottom of the culture chamber shortly before the maximum angle of the rocking platform was reached (red color in Fig 11A and 12A). In horizontal position, the volume-average fluid velocity in the Cellbag culture chamber was approximately two-fold lower. Only in the small region on the wave crest, the fluid velocity reached maximum values comparable with those of the wave crest. The volume-average minimum values were observed shortly before the horizontal position of the rocking platform for both working volumes.

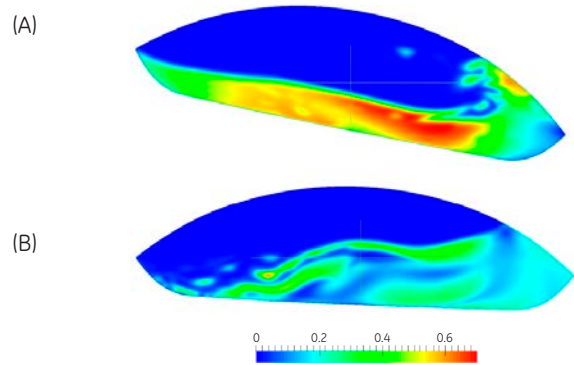


Fig 11. CFD-predicted fluid velocity magnitude pattern in the Cellbag culture chamber with 10 L filling volume at 40 rpm, 12°, and 100% acceleration. Contour plot of velocity magnitude on y - z -plane (side view) at (A) 19.05 s and (B) 19.45 s.

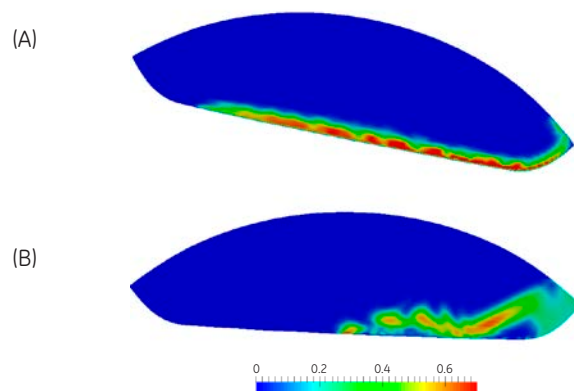


Fig 12. CFD-predicted fluid velocity magnitude pattern in the Cellbag culture chamber with 2 L filling volume at 40 rpm, 12°, and 100% acceleration. Contour plot of velocity magnitude on y - z -plane (side view) at (A) 19.05 s and (B) 19.45 s.

The CFD-predicted profile of the velocity magnitude in the Cellbag culture chamber with 10 L filling volume is illustrated in Figure 13 and with 2 L filling volume in Figure 14. For 10 L filling volume, the acceleration level only affected the fluid velocity profile at lower rocking rates as shown in Figure 13A. At 100% acceleration, the volume-average fluid velocity reached its minimum value before the maximum angle of the rocking platform was reached and the maximum value was in the horizontal position. At 15% acceleration, the profiles were similar at 16 and 20 rpm (Fig 13B and 13C). However, at 10 rpm, the fluid velocity had two minima in horizontal position and at maximum tilt of the rocking platform. At higher rocking rates, a deflection of the fluid velocity profile could be observed: the minimum velocities were observed shortly before the horizontal position and maxima before the maximum tilt of rocking. In addition, the 100% acceleration level resulted in approximately 10% higher fluid velocities compared with the 15% acceleration. For 2 L filling volume, the difference in the fluid velocity due to the acceleration profile could be detected for 10 rpm, 6° and 16 rpm, 8°. For all operating parameters, the fluid velocity is higher with the smaller working volume.

The average and maximum values for the volume-average magnitude of the fluid velocity are listed in Table 3. The average values for fluid velocity increase approximately linearly with higher rocking rates and is higher for the lower filling volume.

For the 10 L filling volume, the increase in rocking rate from 10 rpm to 20 rpm results in an increase in the average velocity from 0.035 to 0.085 m/s. The maximum value of the volume-average fluid velocity rises from 0.065 to 0.135 m/s. The influence of the increasing rocking platform angle on the fluid velocity can be seen by comparing the fluid velocities at 16 rpm and 8° amplitude with 20 rpm and 6° amplitude.

For the lower filling volume of 2 L, the findings are similar. Again, it can be seen that the acceleration has no significant influence on the fluid velocity.

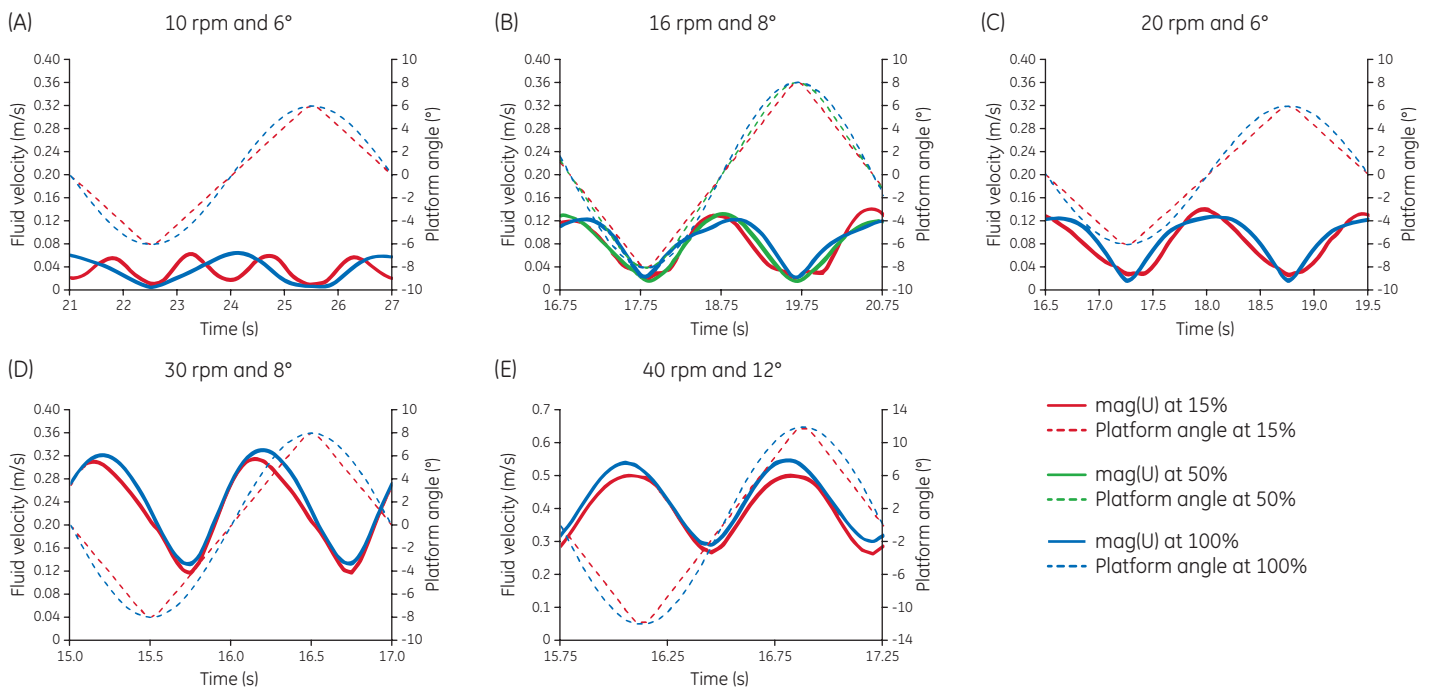


Fig 13. Profiles of the CFD-predicted volume-average magnitude of fluid velocities $\text{mag}(U)$ in the Cellbag culture chamber with 10 L filling volume as a function of time, with 15% (red line), 50% (green line), and 100% (blue line) acceleration.

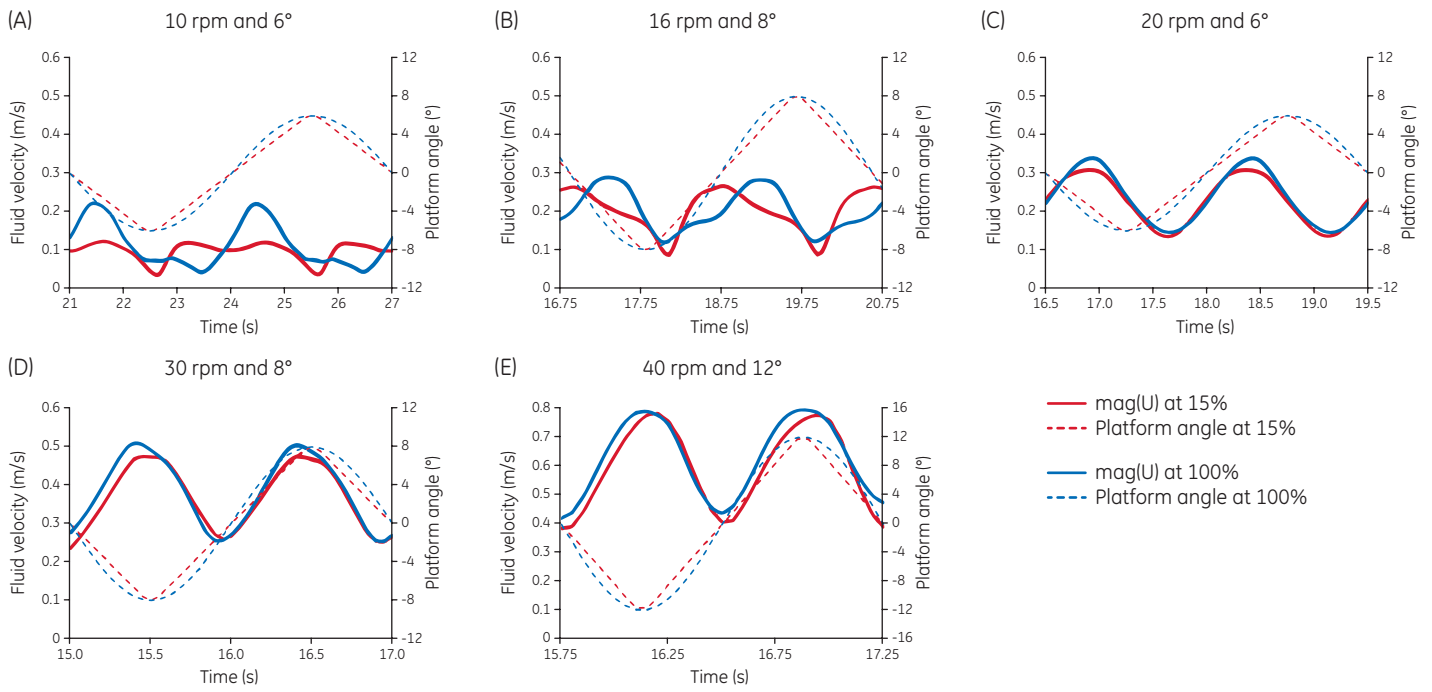


Fig 14. Profiles of the CFD-predicted volume-average magnitude of fluid velocities $mag(U)$ in the Cellbag culture chamber with 2 L filling volume as a function of time, 15% (red line) and 100% (blue line) acceleration.

Table 3. Average and maximum values for CFD-predicted volume-average magnitude of fluid velocity in the Cellbag culture chamber

Rocking speed (rpm)	Rocking speed (°)	Acceleration (%)	10 L		2 L	
			U_{avg} (m/s)	U_{max} (m/s)	U_{avg} (m/s)	U_{max} (m/s)
10	6	15	0.04	0.06	0.10	0.12
10	6	100	0.03	0.07	0.11	0.22
16	8	15	0.07	0.13	0.20	0.27
16	8	50	0.07	0.13	-	-
16	8	10	0.08	0.12	0.20	0.29
20	6	15	0.08	0.14	0.23	0.31
20	6	100	0.09	0.13	0.24	0.34
30	8	15	0.22	0.32	0.37	0.48
30	8	100	0.24	0.33	0.39	0.51
40	12	15	0.40	0.50	0.60	0.78
40	12	100	0.43	0.55	0.63	0.79

Specific power input

The specific power input is one of the most important scaling parameters. Because of the power input mechanism (i.e., the rocking motion), the specific power input is difficult to measure directly without major modifications of the hardware. Therefore, CFD was used to predict power input profiles that can be used in the comparison of cultivation regimes between different bioreactors.

The CFD-predicted profile of the power input in the Cellbag culture chamber with 10 L filling volume is illustrated in Figure 15 and with 2 L filling volume in Figure 16. The profile correlates well with the movement of the rocking platform. The peak values of power input were achieved shortly before and after the maximum tilt of the rocking platform. At 15% acceleration, the power input profile differed from the cosine-shaped power input profile at 100% acceleration and had rectangular peaks, which coincide with the highest angular acceleration of the platform. The peak values of power input directly after the platform rotation reversal were much higher than the peaks before the maximum platform angle was reached, especially at higher rocking rates of 30 rpm and 40 rpm (Fig 15). This observation can be explained by the higher amount of energy required to push back the accelerated fluid that does not reach the end of the Cellbag

culture chamber (see the region with highest fluid velocities in Fig 11A). This phenomenon was not seen at lower rocking rates up to 20 rpm, where the fluid in the bioreactor was in line with the smooth platform movement and thus, in horizontal position, the power input was zero.

The average and maximum values for CFD-predicted specific power input P/V in the ReadyToProcess WAVE 25 bioreactor are listed in Table 4. As expected, higher rocking rates required higher power input and the relationship was not linear. The specific power input at 20 rpm was about 140% higher than at 10 rpm. Higher rocking amplitude required higher specific power input. For example, the required specific power input at 20 rpm and 6° amplitude was 30% higher than at 16 rpm and 8° amplitude.

The filling volume influences the specific power input significantly. For lower rocking speeds, the specific power input was almost three times higher with 2 L working volume, and at higher rocking speed, it was still two-fold higher compared with 10 L filling volume. The highest average specific power input of up to 550 W/m³ for the 2 L filling volume was in good accordance with literature values for smaller-scale rocking bioreactors of 1 L maximal filling volume (around 560 W/m³) (3).

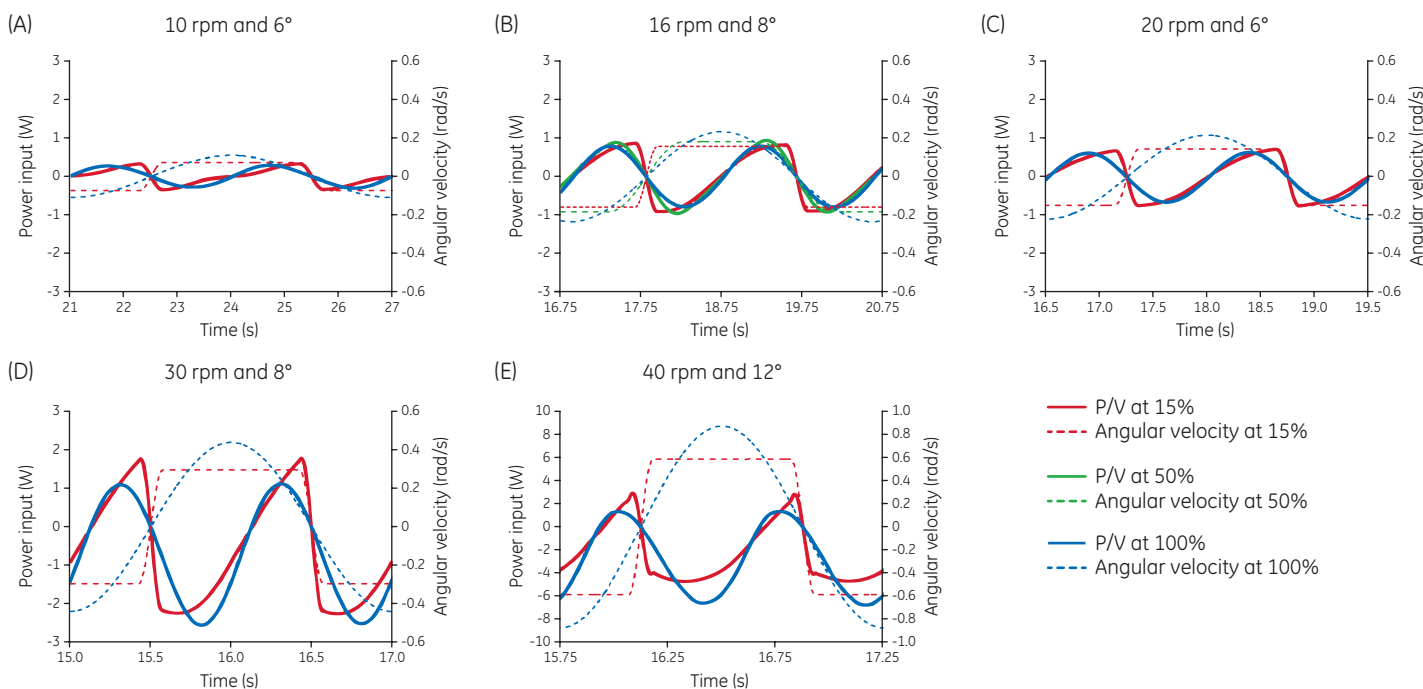


Fig 15. Profiles of the CFD-predicted power input P/V in the Cellbag culture chamber with 10 L filling volume as a function of time, with 15% (red line), 50% (green line), and 100% (blue line) acceleration.

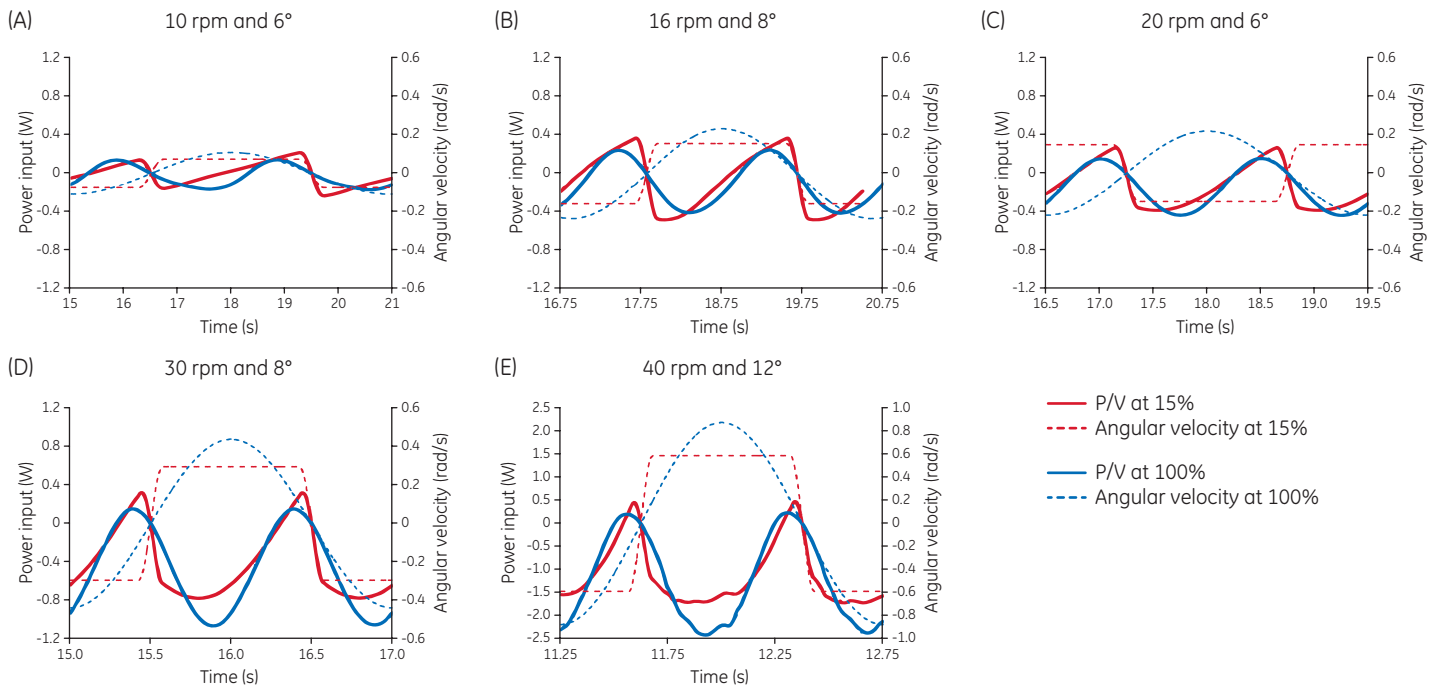


Fig 16. Profiles of the CFD-predicted power input P/V in the Cellbag culture chamber with 2 L filling volume as a function of time, 15% (red line) and 100% (blue line) acceleration.

Table 4. Average and maximum values for CFD-predicted specific power input P/V in the Cellbag culture chamber

Rocking speed (rpm)	Rocking speed (°)	Acceleration (%)	10 L		2 L	
			P/V _{avg} (W/s)	P/V _{max} (W/s)	P/V _{avg} (W/s)	P/V _{max} (W/s)
10	6	15	14.1	34.7	56	118
10	6	100	17.7	30.6	49	86
16	8	15	53.7	94.4	144	240
16	8	50	51.7	100.0	-	-
16	8	10	48.9	81.2	116	250
20	6	15	43.3	75.3	116	194
20	6	100	39.4	65.5	116	221
30	8	15	133.2	225.7	227	389
30	8	100	126.3	255.7	250	533
40	12	15	288.7	474.9	550	861
40	12	100	290.6	680.6	551	1213

Normal stress

The CFD-predicted pattern for normal component of local stress τ_{nn} in the Cellbag culture chamber at 40 rpm, 12° amplitude, and 100% acceleration with 10 L filling volume is presented in Figure 17. The highest values of normal stress were observed close to the bag wall. When the rocking platform was passing through the horizontal position, a region with high normal stress of about 10 mPa occurred where the returning wave fell down. The CFD-predicted volume-average normal stress in the Cellbag culture chamber with 10 L filling volume is illustrated in Figure 18 and with 2 L filling volume in Figure 19. The lowest volume-average values for normal stress could be observed, especially at lower rocking rates, when the rocking platform reached the maximum angle. The highest volume-average values were observed in horizontal position. This finding correlates well with the fluid velocity profile. Interestingly, slightly higher fluctuations could be observed at 15% acceleration level compared with 100% acceleration, which could be explained with the higher angular accelerations of the rocking platform at 15% acceleration. At higher rocking rates of 30 rpm and 40 rpm, the volume-average values fluctuated strongly. This could be explainable by the effect of high turbulence in the bioreactor.

The filling volume influenced the normal stress values in a similar manner as it influenced the fluid velocity and power input, with a two- to three-fold increase for 2 L compared with 10 L filling volume. Higher fluid velocities within the

culture chamber with 2 L filling volume explain the higher values of stress. The maximum values of CFD-predicted volume-average normal stress were lower than 10 mPa. Also the CFD-predicted cell-maximum values (which occurred in a very small volume of one CFD mesh cell only) for normal stress were about 1.3 Pa and 2.1 Pa at 30 rpm and 40 rpm, respectively.

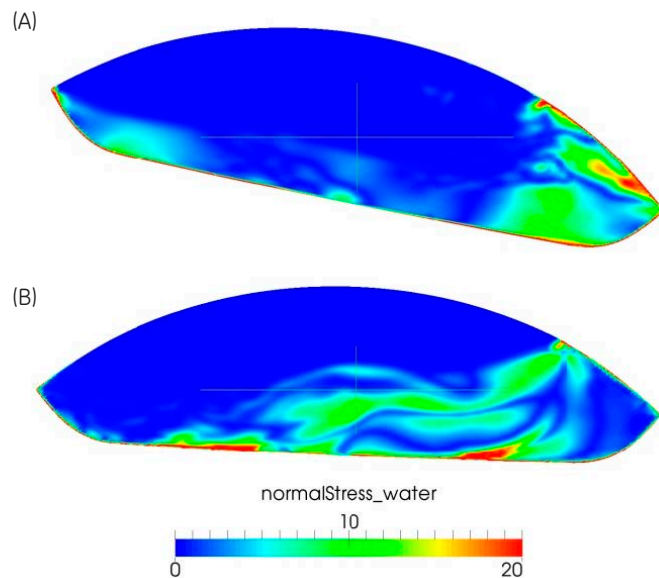


Fig 17. CFD-predicted normal stress pattern in the Cellbag culture chamber with 10 L filling volume at 40 rpm, 12°, and 100% acceleration. Contour plot of velocity magnitude on y-z-plane (side view) at (A) 19.05 s and (B) 19.45 s.

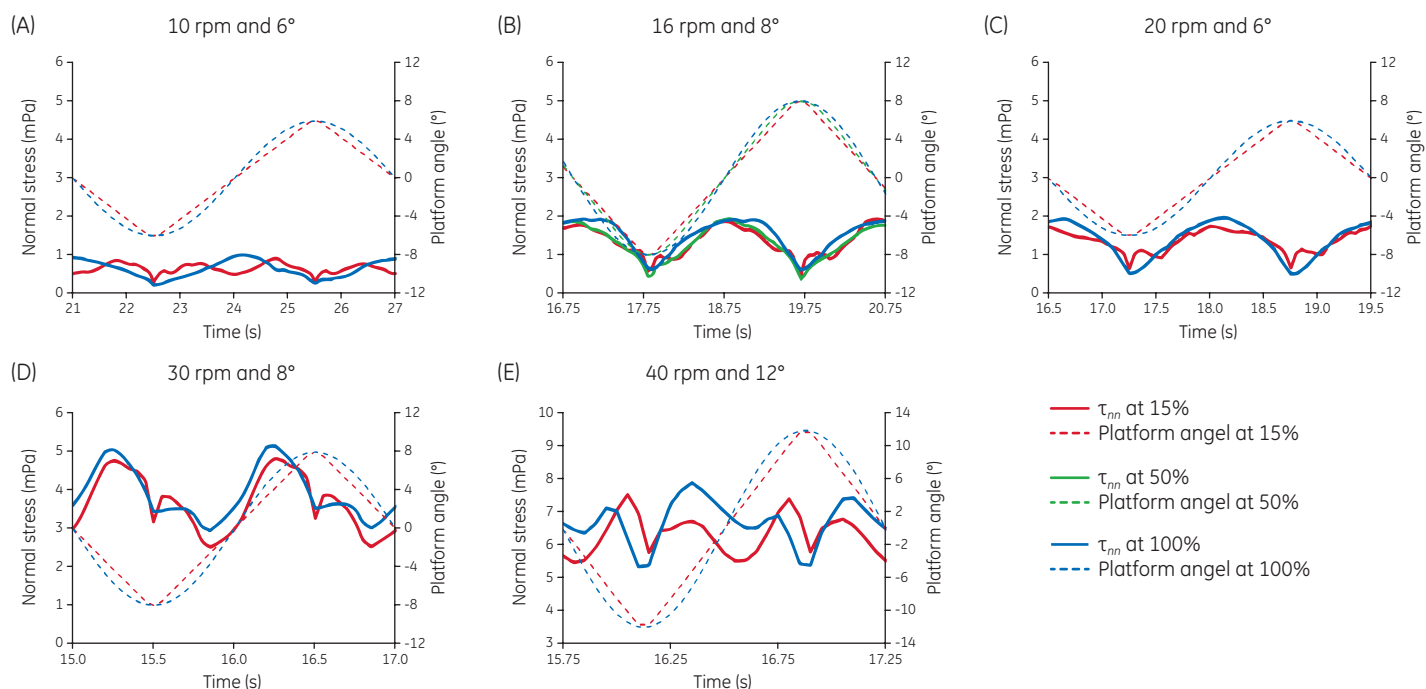


Fig 18. Profiles of the CFD-predicted volume-average normal stress in the Cellbag culture chamber with 10 L filling volume as a function of time, 15% (red line), 50% (green line), and 100% (blue line) acceleration.

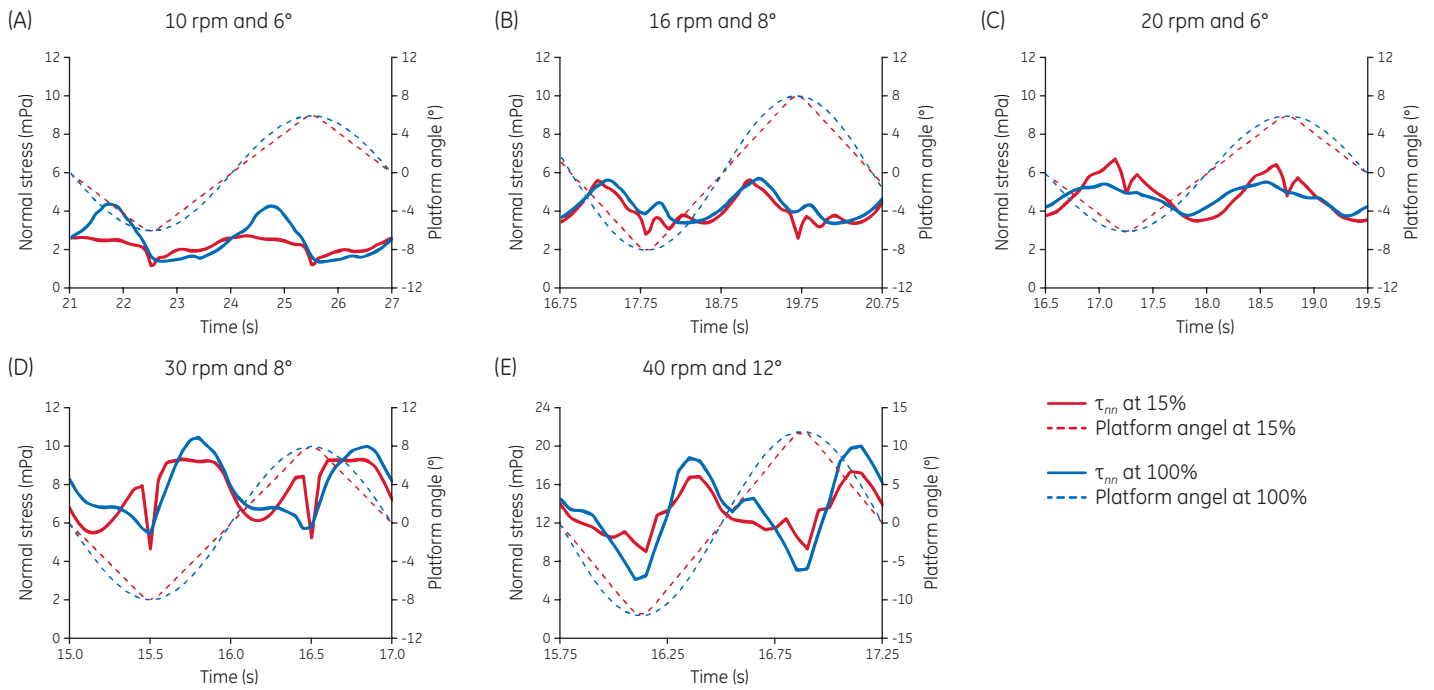


Fig 19. Profiles of the CFD-predicted volume-average normal stress in the Cellbag culture chamber with 2 L filling volume as a function of time, 15% (red line) and 100% (blue line) acceleration.

Shear stress

The CFD-predicted pattern for the shear component τ_{nt} of local stress in the Cellbag culture chamber at 40 rpm, 12° amplitude, and 100% acceleration with 10 L filling volume are presented in Figure 20. As expected, the CFD-predicted shear stress exceeded the normal stress approximately by a factor of two. The shear stress is suspected to cause higher cell damage than normal stress (7). As for normal stress, shear stress is found to be highest at the walls of the culture chamber. In addition, values about of 20 to 30 mPa (green color Figure 20) can be observed in front of the wave crest.

The CFD-predicted volume-average shear stress in the Cellbag culture chamber with 10 L filling volume is illustrated in Figure 21 and with 2 L filling volume in Figure 22. The oscillations observed at 10 rpm, 6° amplitude, and 15% acceleration level correlate well with fluid velocity profile (compare Fig 2 and 15). Like for normal stress, the lowest volume-average values for shear stress can be observed, especially at lower rocking rates (up to 20 rpm), when the rocking platform reaches the maximum angle. The highest volume-average values are achieved in the horizontal position. At higher rocking rates of 30 and 40 rpm, the volume-average values at 100% acceleration level are 9% to 12% higher than at 15% acceleration (Fig 21).

The CFD-predicted cell-maximum values for shear stress with 10 L working volume were about 6.5 Pa and 9.1 Pa at 30 rpm and 40 rpm, respectively. These values are higher with lower working volume.

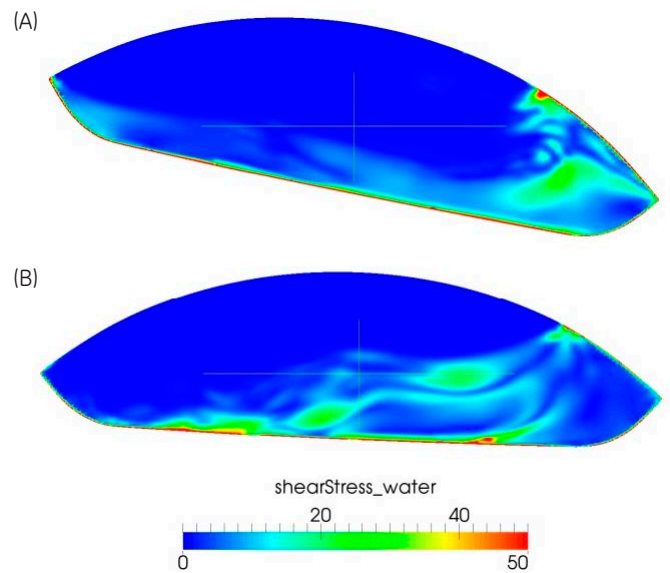


Fig 20. CFD-predicted shear stress pattern in the Cellbag culture chamber with 10 L filling volume at 40 rpm, 12°, and 100% acceleration. Contour plot of velocity magnitude on y-z-plane (side view) at (A) 19.05 s and (B) 19.45 s.

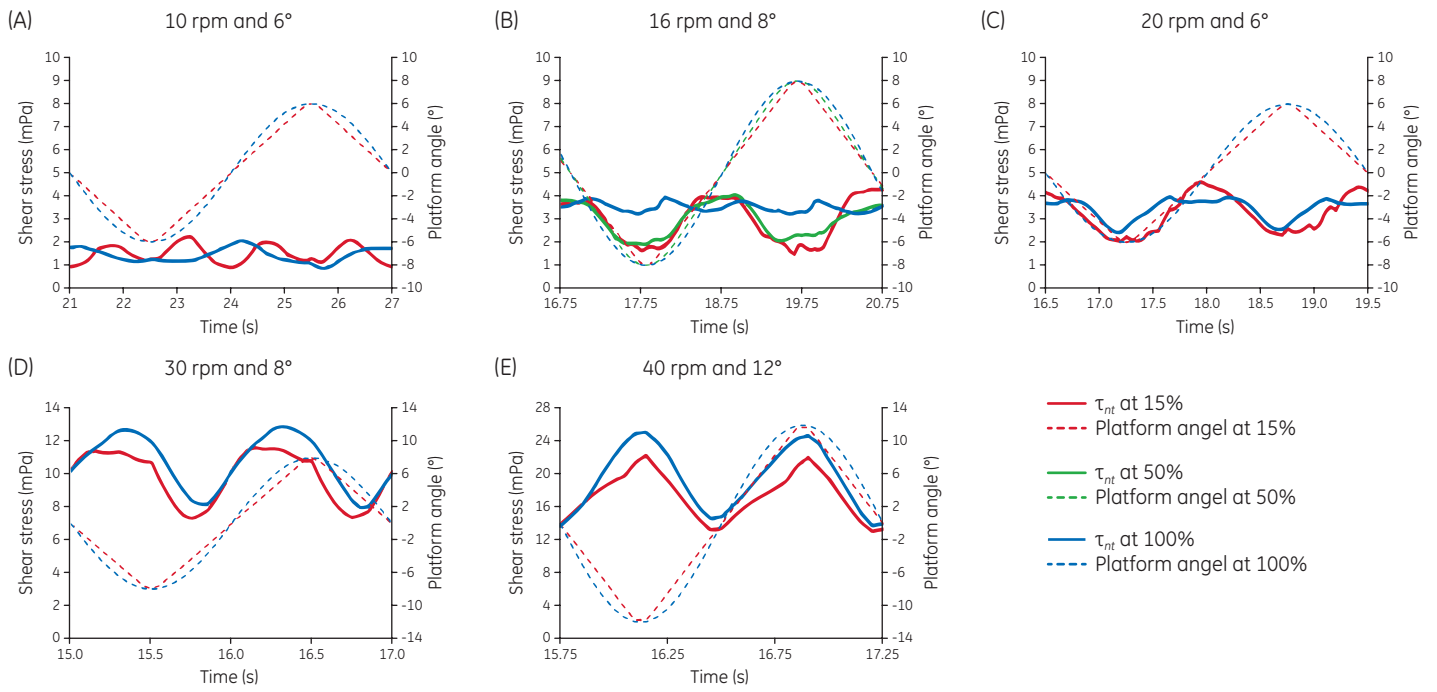


Fig 21. Profiles of the CFD-predicted volume-average shear stress in the Cellbag culture chamber with 10 L filling volume as a function of time, 15% (red line), 50% (green line), and 100% (blue line) acceleration.

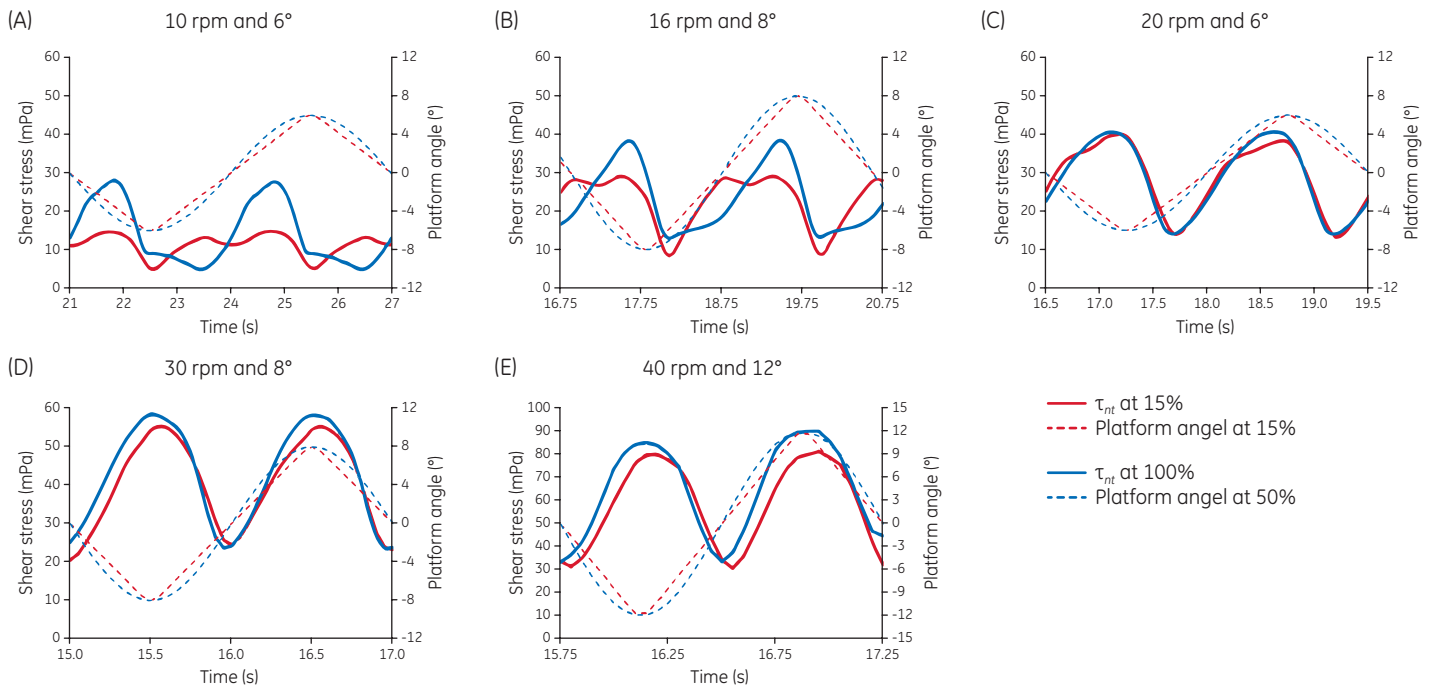


Fig 22. Profiles of the CFD-predicted volume-average shear stress in the Cellbag culture chamber with 2 L filling volume as a function of time, 15% (red line) and 100% (blue line) acceleration.

Kolmogorov microscale of turbulence

The microscale of turbulence is often considered as an indicator of possible cell damage. Cells in a bioreactor are damaged by the turbulence eddies of comparable sizes (6, 8–10).

As shown in Figure 23, the values of the microscale of turbulence in the Cellbag culture chamber at 10 rpm/6°, 16 rpm/8°, and 20 rpm/6° are higher than 100 μm, which is significantly larger than the size of a mammalian cell. With

the increase of the rocking rate, the size of the turbulence eddy decreases. At higher rocking rate the turbulence is stronger and the eddy size is in the range of a plant cell: around 55 μm at 30 rpm/8° and around 40 μm at 40 rpm/12°. Furthermore, it can be seen, that the volume-average values for the microscale of turbulence are only slightly changing over time, independent from the acceleration level of the rocking platform.

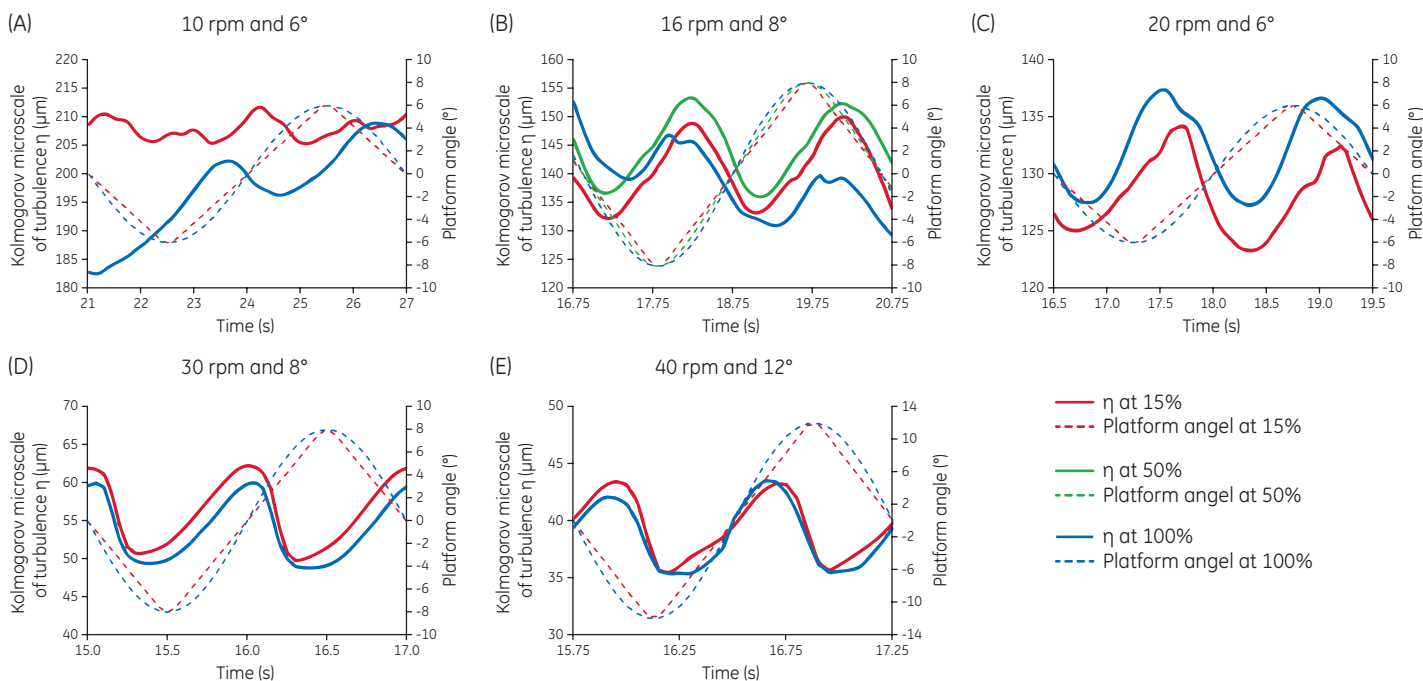


Fig 23. Profiles of the CFD-predicted volume-average Kolmogorov microscale of turbulence η in the Cellbag culture chamber with 10 L filling volume as a function of time, 15% (red line), 50% (green line), and 100% (blue line) acceleration.

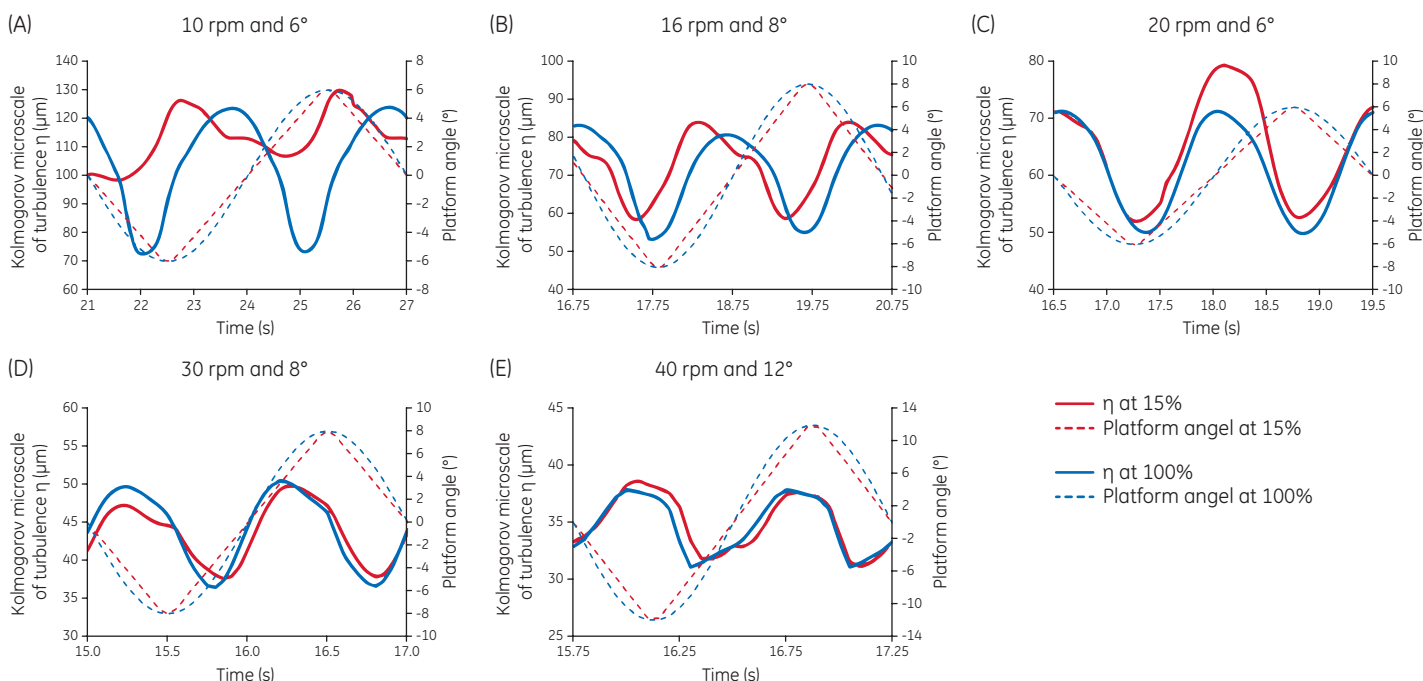


Fig 24. Profiles of the CFD-predicted volume-average Kolmogorov microscale of turbulence η in the Cellbag culture chamber with 2 L filling volume as a function of time, 15% (red line) and 100% (blue line) acceleration.

For low working volumes of 2 L, the microscale of turbulence is in the cell size range even at low rocking speed and angle (Fig 24). Here, it is recommended to start a culture at a low rocking speed of only 10 rpm and 6° angle. Experimental investigations showed that at low working volume, even using lowest operating parameters, ensures oxygen mass transfer rates of around 4.5 h⁻¹, which is sufficient for many applications. However, important to note is that the calculation was done with water-like fluid properties.

Conclusions

The investigation of the engineering characterization (mixing time and oxygen mass transfer rate) of the ReadyToProcess WAVE 25 was done with a Cellbag 20 L with 2 L and 10 L working volume. Our results show that rocking speed and angle have the highest influence on mixing time and oxygen mass transfer rate. At the same rocking speed and angle, the acceleration has an influence on the mixing time at lower rocking speeds up to 20 rpm.

The volume-average and the maximum values for the fluid velocity, the specific power input, the normal and shear stress, and the Kolmogorov microscale of turbulence in the Cellbag culture chamber for the operating parameters were calculated for every time step. The CFD simulation shows that the acceleration parameter only has little influence on calculated parameters. Rocking speed and angle were shown to influence the fluid flow behavior, and even more, the filling volume was shown to have a significant influence on the fluid flow parameters.

Acknowledgement

We thank Sören Werner, Mischa Stalder, Nadezda Perepelitsa, and Dieter Eibl at the Zurich University of Applied Sciences for sharing of data.

References

1. Löffelholz, C. Husemann, U. Greller, G. Meusel, W. Kauling, J. Ay, P. Kraume, M. Eibl, R. Eibl, D. Bioengineering parameters for single-use bioreactors: overview and evaluation of suitable methods. *Chemie Ingenieur Technik* **85**, 40-56 (2013).
2. Eibl, R., Werner, S., and Eibl, D. Bag bioreactor based on wave-induced motion: characteristics and applications. *Advances in biochemical engineering/biotechnology* **115**, 55-87 (2010).
3. Eibl, R., Werner, S., and Eibl, D. Disposable bioreactors for plant liquid cultures at litre-scale. *Engineering in Life Sciences* **9**, 156-164 (2009).
4. Krause, B. Strömungsabhängige Darstellung des Tensors der Geschwindigkeitsgradienten. In 10. Köthener Rührerkolloquium, pp 62-71, Köthen (2007).
5. Wollny, S. Experimentelle und numerische Untersuchungen zur Partikelbeanspruchung in gerührten (Bio-)Reaktoren. Dissertation, Technische Universität Berlin (2010).
6. Werner, S., Greulich, J., Geipel, K., Steingroewer, J., Bley, T., and Eibl, D. Mass propagation of *Helianthus annuus* suspension cells in orbitally shaken bioreactors: Improved growth rate in single-use bag bioreactors. *Engineering in Life Sciences* **14**, 676-684 (2014).
7. Langer, G. and Deppe, A. Zum Verständnis der hydrodynamischen Beanspruchung von Partikeln in turbulenten Rührerströmungen. *Chemie Ingenieur Technik* **72**, 31-41 (2000).
8. Löffelholz, C., Kaiser, S.C., Werner, S., and Eibl, D. CFD as tool to characterize single-use bioreactors. In *Single-use technology in biopharmaceutical manufacture* (Eibl, R. and Eibl, D. eds.), pp. 263-279. John Wiley & Sons, Inc., Hoboken, NJ, USA (2011).
9. Chisti, Y. Hydrodynamic damage to animal cells. *Critical reviews in biotechnology* **21**, 67-110 (2001).
10. Kolmogorov, A.N., Limberg, H., and Goering, H. *Sammelband zur statischen Theorie der Turbulenz*. Akademie-Verlag, Berlin (1958).

gelifesciences.com/wave

GE, GE monogram, Cellbag, ReadyToProcess WAVE, and UNICORN are trademarks of General Electric Company. Any use of UNICORN software is subject to GE Healthcare Standard Software End-User License Agreement for Life Sciences Software Products. A copy of this Standard Software End-User License Agreement is available on request.
© 2016 General Electric Company. First published Aug. 2016.
All goods and services are sold subject to the terms and conditions of sale of the company within GE Healthcare which supplies them. A copy of these terms and conditions is available on request. Contact your local GE Healthcare representative for the most current information.
GE Healthcare UK Ltd., Amersham Place, Little Chalfont, Buckinghamshire, HP7 9NA, UK
GE Healthcare Europe GmbH, Munzinger Strasse 5, D-79111 Freiburg, Germany
GE Healthcare Bio-Sciences Corp., 100 Results Way, Marlborough, MA 01752, USA
GE Healthcare Dharmacon Inc., 2650 Crescent Dr, Lafayette, CO 80026, USA
HyClone Laboratories Inc., 925 W 1800 S, Logan, UT 84321, USA
GE Healthcare Japan Corp., Sanken Bldg., 3-25-1, Hyakunincho Shinjuku-ku, Tokyo 169-0073, Japan
For local office contact information, visit gelifesciences.com/contact.